https://doi.org/10.48048/tis.2023.6520

DFT Study on the Molecular Mechanism, Thermodynamic and Kinetic Parameters of Cycloaddition Reaction of Aziridine with CO_2 in the Presence of Organocatalysts (TBD and 7-Azaindole)

Tesfaye Tadesse Gebre[1], Teshome Abute Lilisho[2] and Birhanu Bekele Gosa[1,*]

[1]Department of Chemistry, College of Natural and Computational Science, Bonga University, Bonga, Ethiopia
[2]Department of Chemistry, College of Natural and Computational Science, Hawassa University, Hawassa, Ethiopia

([*]Corresponding author's e-mail: birhanu214@gmail.com)

Received: 1 October 2021, Revised: 11 November 2021, Accepted: 21 November 2021, Published: 26 December 2022

Abstract

The catalytic conversions of CO_2 into value added chemicals have attracted the interest of many visionary researchers. In this work, the coupling reaction of aziridine with CO_2 has been investigated in the absence and presence of organocatalysts (TBD and 7-azaindole) computationally using density functional theory method. The kinetic and thermodynamic parameters of each mechanism were calculated at B3LYP/6-31G (d) level. The results show that, the TBD and 7-azaindole catalyzed reactions of aziridine with CO_2 have significantly lower the energy barrier compared to a single step concerted non-catalyzed one. In TBD catalyzed reaction, mechanism I in which the TBD catalyst first interact with CO_2 to form TBD-CO_2 adduct (zwitterion) and then the zwitterion formed facilitated the ring opening of aziridine to form intermediate is the favorable path. In the case of 7-azaindole catalyzed reaction, mechanism 1 is the most favorable pathway in both gas phase and water phase. However, these parameters were significantly affected in the presence of water using Solvent Model Density (SMD).

Keywords: Cycloaddition, Carbon dioxide, Aziridine, Trazabicyclodecene, 7-azaindole, TBD, Zwitterion, Coupling reaction

Introduction

Energy is an important component for sustainable economic development. Global demand for energy is increasing rapidly as a result of population and economic growth. An obvious consequence of this is an increase in the use of fossil fuels, particularly conventional energy demand is extracted from nonrenewable energy source (fossil fuel) like coal, crude oil, natural gas, nuclear fuel have become key energy sources since the industrial revolution. Humans extract them in gas, liquid, or solid form and then convert them for their use, mainly related to energy [1-4]. Currently, fossil fuel combustion is the main source of energy that yields carbon dioxide as by product. Emissions of CO_2 from anthropogenic activities accounts for approximately 95 % of the total global annual CO_2 emissions [6]. However, the abundant use of fossil fuels has become anxiety concern due to their adverse effects on the environment, particularly related to the emission of anthropogenic greenhouse gas carbon dioxide [5]. The emission of carbon dioxide into the atmosphere is recognized as the main reason for climate change and its secondary effects including global warming, changes in sea levels, extreme hot summers and cold winters, and agricultural problems. Transforming of carbon dioxide to useful value added chemicals has attracted the attention because it could reduce the dependence on diminishing fossil as well as mitigate CO_2 emission [5-7]. The chemical fixation of CO_2 for various synthetic transformations is a hot topic in current researches. It is an attractive method because there are many possibilities for CO_2 to be used as a safe and cheap C1 building block in organic synthesis. One of the most meaningful and environment-friendly ways for this procedure is the cyclic carbonates synthesis via the coupling reaction of aziridine with CO_2 [7,8]. Oxazolidinone is a 5-member heterocyclic ring compound exhibiting potential medicinal properties with preferential antibacterial activity [9]. It is a new class of antimicrobial agents which have a unique structure and good activity against gram-positive pathogenic bacteria. Current review articles tried to cover each and every potential aspect of oxazolidinone like synthetic routes, pharmacological mechanism of action, medicinal properties, and current research activities [10]. So thermodynamic stability and kinetic inertness of CO_2 hinder the development of efficient catalysts that achieve CO_2 activation and its

.

subsequent functionalization. However, the exploration of highly efficient catalysts for CO_2 coupling with aziridine under mild conditions still remains a challenging task. Among different carbon capture and storage (CCSs) method, post combustion capture using chemical absorption is considered to be a promising new approach to mitigate CO_2 emission. In recent years, amine based solvents are widely used for CO_2 capture from industrial flue gases. Various amine based solvents were tested so far in order to obtain solvents with good absorption and low regeneration energy [11]. Great efforts have been devoted to design amine based solvents in order to obtain solvents with good absorption and low regeneration energy. However, because of some draw backs, this technology is not yet properly implemented in large scale so as to mitigate the greenhouse. One of the challenging problems in this technology is high energy demand for the regeneration step. Another proposal involves chemical fixation of CO_2. Chemical fixation of CO_2 into value added compounds imparts paramount advantages in organic synthesis attributed to its non-toxicity, abundance, non-flammability and cheapness. Extensive efforts have been done to use CO_2 as C1 building block like conversion into formic acid, methnol and cyclic carbonates [12]. In particular the chemical fixation of with aziridine to produce oxazolidinone is a promising synthetic strategy. Despite its enormous potential benefits, chemical fixation of CO_2 to oxazolidinone remains a formidable challenge due to thermodynamic stability and kinetic inertness of CO_2 in its highly oxidized form. So far, numerous catalytic systems like alkali metal salt, ionic liquids, naturally occurring ά-amino acids and organocatalysts were reported to be effective for the couple reaction of CO_2 with aziridine. However, the exploration of highly efficient catalysts for CO_2 coupling with aziridines under mild conditions still remains a challenging task. Furthermore, the reaction mechanism is also debatable. Thus, in this study 2 organocatalysts (TBD and 7-AZ) were selected to test whether these species facilitate the coupling reaction or not.

Materials and methodology

Computational details

All quantum chemical calculations were performed by using density functional theory method with Becke's 3-parameter hybrid exchange functional and the Lee-Yang-Parr [13,14] correlation functional at B3LYP/6-31G(d) level of theory included within the Gaussian 09 package [15,16]. Gauss view 5.0.9 was used to prepare input for submission to Gaussian and to examine graphically the output that Gaussian calculates. The geometries structures of the reactant complexes (RC), intermediates (IM), product complexes (PC) and saddle points (transition states). Transition states were allocated by using quadratic synchronous transit (QST3) methods was applied to obtain the structures of transition states. This technique requires supplying structures for the complex of reactants and the complex of products, and a guess of the transition state geometry and predicts mechanism. Vibrational frequency calculations were conducted to check the local minima (with real frequency) and saddle point (one imaginary frequency) by opening the output file of optimized geometries. Intrinsic reaction coordinate (IRC) is used to confirm the relationship between the transition states as well as the reactants and products. Solvent Model Density (SMD) model was employed in order to investigate solvent effect on the reaction mechanism, kinetic and thermodynamic properties. It is a universal solvation model, where "universal" denotes its applicability to any charged or uncharged solute in any solvent or liquid medium for which a few key descriptors are known (in particular, dielectric constant, refractive index, bulk surface tension and acidity and basicity parameters [17]. This model has a root of mean squared (RMS) error for polar protic solvent has 3.0 kcal/mol and good performance to predict free energy of activation of neutral and anion molecule reactions [18]. Electrophilic Pk+ and nucleophilic Pk- Parr functions [19] were obtained through the analysis of the Mulliken atomic spin density of the corresponding radical cations or anions, respectively, and calculated as $\omega_A = \omega . P^+{}_A$ and $N_A = N . P^-{}_A$, respectively. The electrophilicity index (ω), nucleophilicity index, chemical potential (μ) and chemical hardness were calculated as:

$$\omega = \frac{\mu^2}{2\eta} \quad (1)$$

$$\mu = \frac{\varepsilon_{HOMO} + \varepsilon_{LUMO}}{2} \quad (2)$$

$$N = \varepsilon_{HOMO\ (NU)} - \varepsilon_{HOMO\ (TCE)} \quad (3)$$

$$\eta = \varepsilon_{\mathrm{LUMO}} - \varepsilon_{\mathrm{HOMO}} \quad (4)$$

The global electron density transfer (GEDT) [20] is computed by the sum of the natural atomic charges (q), obtained by a natural population analysis (NPA) [21] of the atoms belonging to each framework (f) at the transition state.

Results and discussion

Cycloaddition reaction between aziridine and carbon dioxide without catalyst

In order to explore the catalytic role of TBD and 7-AZ, we have investigated plausible pathway for the coupling reaction between CO_2 and aziridine in the absence of the catalysts. We proposed a mechanism for the coupling reaction between CO_2 and aziridine in the absence of the catalyst based on the related work of Li *et al.* [22] and it is a 2-step pathway as shown in **Figure 1**. Li *et al.* [22] reported the mechanism for the chemical fixation of CO_2 with N-benzylaziridine catalyzed by N-heterocyclic carbine (NHC). In this paper, 3 possible pathways are reported for uncatalyzed pathway in which the reaction begins from the formation of ternary complexes. In this ternary complex (reactant complex of 2 N-benzylaziridine molecules and 1 CO_2 molecule), CO_2 is weakly interacting with N atom of 1 N-benzylaziridine, which facilitated the ring opening of aziridine to form zwitterions intermediate. According to the authors, the ring opening occurred when the N atom of other N-benzylaziridine attacks C atom of the aziridine to form the intermediate.

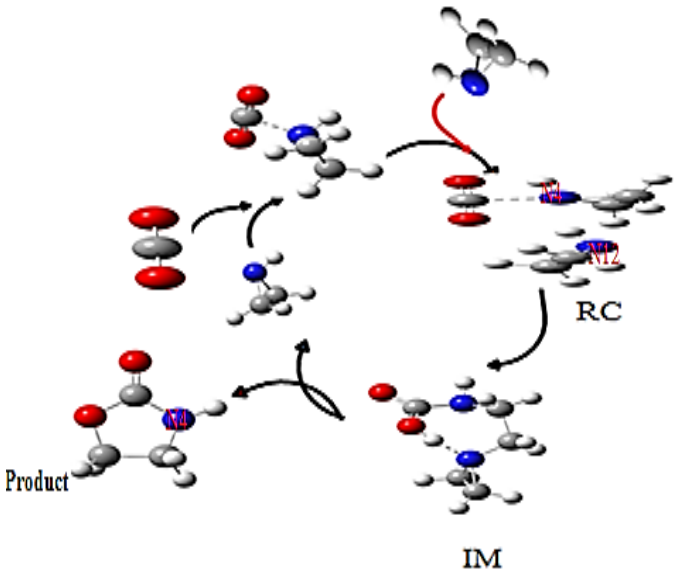

Figure 1 Proposed reaction mechanism of CO_2 with 2 aziridine in the absence of TBD and 7-AZ.

Using similar approach of Li *et al.* [22], we proposed the mechanism for the coupling reaction for 2 aziridine molecule and 1 carbon dioxide as indicated in **Figure 1**. To begin this mechanism, the PES using redundant coordinate was carried out first by varying the distance between C of CO_2 and N of aziridine at B3LYP/6-31G(d) level to check whether the zwetterion exists or not, when CO_2 and aziridine interact with each other. We obtained only 1 valley. The structure from the minima of PES was taken and further optimized at the same level of theory. The structure obtained is shown on the electronic supplementary information **Figure 1** and we couldn't found the zwetterion for aziridine-CO_2 system. We proposed probable pathway for this mechanism and the suggested mechanism herein involves 2 elementary steps: Intermediate formation and intramolecular nucleophilic addition as shown in **Figure 1**. The potential energy profile for this reaction pathway is presented in **Figure 2** together with the optimized structures of the species involved. In the first step, the reaction begins from the formulation of reactant complex in which CO_2 is weakly interacting with the nitrogen atom of one of reactant complex (RC), N from the second aziridineleads the formation of intermediate (IM).

Table 1 Thermodynamic and kinetic parameters of the reaction of 2 aziridine molecules with carbon dioxide at B3LYP/6-31G (d) in gas phase (Energy in kcal/mol, ΔS in cal/mol·K and k(T) in S^{-1}.

Thermodynamic data			Kinetic data		
	RC→IM	**IM→PC**		**RC→IM (TS1)**	**IM→PC (TS2)**
ΔE(T)	−24.405	−23.551	$\Delta E^{\neq}$	37.0174	66.223
ΔH	−24.405	−23.551	$\Delta H^{\neq}$	37.017	66.223
ΔG	−16.305	−17.653	$\Delta G^{\neq}$	42.968	64.693
ΔS	−27.17	−19.785	$\Delta S^{\neq}$	−19.962	5.132
(Keq)	8.97×10^{11}	8.73×10^{12}	k(T)	1.97×10^{-19}	2.33×10^{-35}

Note: RC = reactant complex, IM = intermediate, PC = product complex

Transition states were located linking the RC to IM and IM to PC at the same level. The formation of IM from RC through transition state 1 (TS1) is exothermic by −24.405 kcal/mol in gas phase, with an activation energy barrier of 37.02 kcal/mol and the activation barrier for the transformation from IM to PC through TS2 is 66.22 kcal/mol, indicating that the second step is rate determining. As can be seen from **Table 1**, the calculated free energy change values for the conversion of RC to IM and IM to PC, respectively are −16.305 and −17.653 kcal/mol. These suggest that the coupling reaction of aziridine with CO_2 is spontaneous and thermodynamically favorable in the forward direction. As depicted in **Figure 1**, the second aziridine is regenerated in the second step, implying that aziridine is acting as a catalyst here.

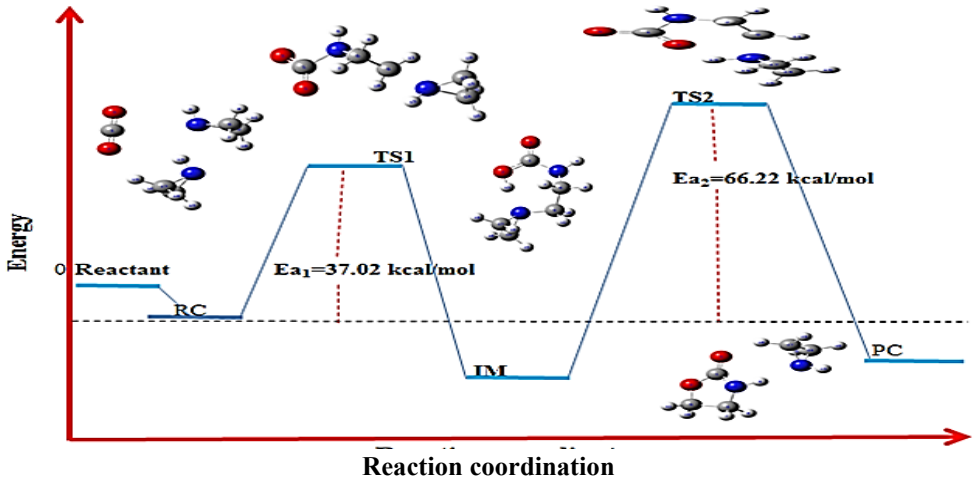

Figure 2 Potential energy profiles for reaction of CO_2 with 2 aziridine in gas phase.

The rate constant predicted for the formation of IM from RC is 1.97×10^{-19} s^{-1}. Similarly k(T) value obtained for the second step is 2.33×10^{-35} s^{-1}. The calculated kinetic data show that, the rate of coupling of CO_2 with azirdine in the absence of catalyst is slow. Whereas the culaculated thermodynamic data (ΔH, ΔG and Keq) imply the forward CA reaction is thermodynamically favorable. The calculated kinetic data as given in **Table 1** for the proposed mechanism suggest that the coupling reaction of CO_2 with aziridine under ordinary condition is unlikely and thus catalyst is required.

Cycloaddition reaction of aziridine with CO_2 in the presence of TBD organocatalyst

Recently, organocatalysis has attracted the interest of many researchers because organocatalyst possess the merits of lowcost, low-toxicity and high stability and can thus be considered as competitive alternatives to their metal counterpart [23]. Among organocatalyst,triazabicyclodecene(1,5,7 Triazabicyclo [4.4.0] dec-5-ene (TBD) is the most widely studied catalyst and has been reported to successfully accelerate various reactionssuch as aminolysis of esters [24], synthesis of cyanohydrin

carbonates [25], cyanosilylation of aldehydes and ketones, Michael reaction, Aldol reaction to list few. It was because of unique nature of TBD we decided to investigate TBD as the catalyst system in this thesis in order to validate whether it is a good candidate to facilitate the reaction or not. Based on the survey of related literature and calculated global and local reactivity descriptors, we proposed 2 hypothetical mechanisms (mechanism 1 and mechanism 2) for TBD catalyzed reaction of aziridine with CO_2 as depicted in **Figures 7** and **11**. To verify the proposed mechanisms, analyses of the local reactivity indices are used to indicate the most electrophilic and nucleophilic centers of the reactant **Tables 2** and **3**.

Table 2 Electronic chemical potential, chemical hardness, global nucleophilicity and global electrophilicity of aziridine, CO2 and TBD catalyst (TCEHOMO = −0.3352 hartree).

Compounds	E_{HOMO}	E_{LUMO}	μ (ev)	η (ev)	N (ev)	ω (ev)
Aziridine	−0.24382	0.08026	−2.225	8.819	2.487	0.281
CO2	−0.36997	0.02991	−4.627	10.88	−0.95	0.984
TBD	−0.19197	0.0516	−1.91	6.628	3.897	0.275

From **Table 2** the large global electrophilicity index value of CO_2 (0.984 ev) indicates the capability CO_2 to accept electrons. Large nucleophilicity indexes of aziridine and TBD indicate the higher capability of these species to donate electrons.

Table 3 Parr functions for aziridine, carbon dioxide and TBD.

TBD	Pk-	Aziridine	Pk-	CO_2	Pk+
C1	−0.0291	C1	0.107307	C1	0.69196
C2	−0.1222	N4	0.735217	O2	0.15402
C3	−0.0092	C6	0.107286	O3	0.15402
C4	0.00628				
N11	0.62207				
N12	0.24108				
C13	−0.0151				

Calculated nucleophilic parr function (Pk-) for TBD and aziridine and electrophilic parr (Pk+) function for CO_2 are summarized in **Table 3**. Nucleophilic Parr function (Pk-) for N11 (0.62207) of TBD and N4 (0.735217) of aziridine are very large. Similarly, electrophilic parr function (Pk+) for C1 (0.69196) of CO_2 was very large. The values of the Parr functions indicate that atom number C1 is electrophilic center in carbon dioxide molecule and N11 and N4 are nucleophilic centers of TBD and aziridine respectively. From the **Figure 3**, the calculated HOMO-LUMO gap value (10.88129 ev) for CO_2 is large. The larger HOMO-LUMO gap always refers to higher kinetic stability and lower chemical reactivity. In addition, the frontier molecular orbitals of these 3 compounds are at the "frontier" of electron occupation in the highest energy occupied and lowest-energy unoccupied molecular orbitals (HOMO and LUMO). The HOMO is logically viewed as nucleophilic or electron donating in TBD and aziridine, while the LUMO is electrophilic and electron accepting in CO_2.

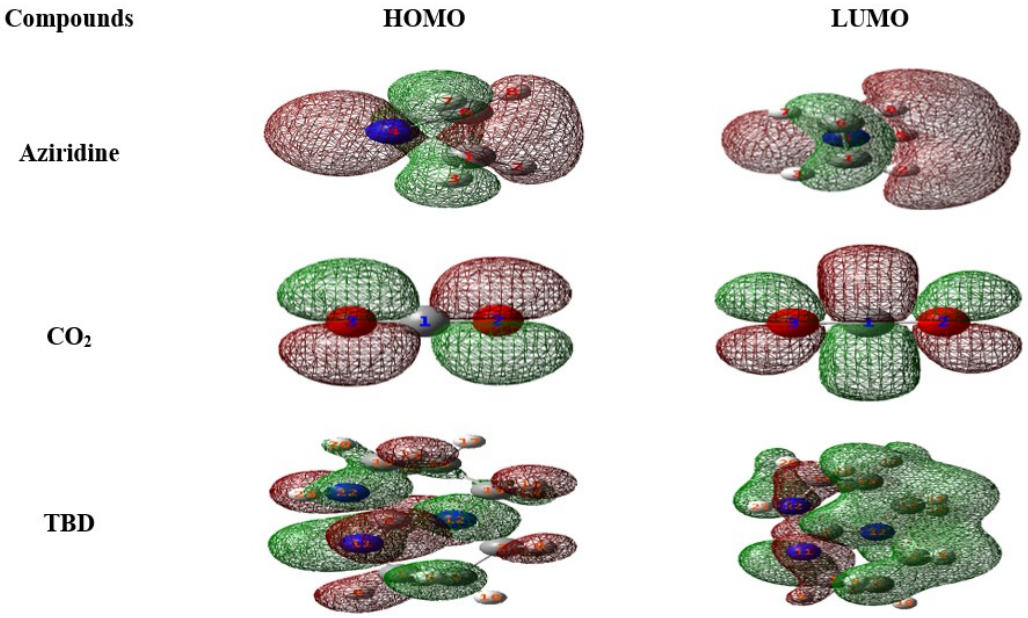

Figure 3 HOMO-LUMO structures for the TBD, aziridine and CO_2.

Reaction mechanism 1

Based on the analysis of global and local descriptors of TBD, aziridine and CO_2 and survey of related works, we proposed the first hypothetical reaction mechanism (mechanism 1) as presented in **Figure 7**. As shown in the scheme, this mechanism involves likely elementary reaction steps for coupling of CO_2 with aziridine catalyzed by TBD. These steps can be followed as first TBD-CO_2 adduct (zwitterion) formation can takes place. Next the ring opening of aziridine with CO_2 moiety of TBD-CO_2 adduct (zwitterion) can form. Then finally a ring closure step was formed.

Step I: TBD-CO_2 adduct (zwitterion) formation

The reaction mechanism for absorption of CO_2 with aqueous amine solvent is still debatable. Some group proposes formation of zwitterion and others propose the termolecular mechanism. The formation of zwitterions mechanism was originally proposed by Caplow (1968) and consists of 2-step mechanism, i.e. the reaction between CO2 and the acap; owmine proceeds through the formation of zwitterion as the first step. Initially, the relaxed PES scan using redundant coordinate was carried out at the B3LYP/6-31G(d) in gas phase in order to explore the nature of interactions between TBD and CO_2, by varying bond distance between N14 of TBD and C1 of CO_2. Two valleys (A and B) in the PES were observed and therefore 2 stable structures are predicted as depicted in **Figure 4**. The 2 structures were further optimized at the same level without symmetry constraint. The harmonic frequency calculations for the 2 structures yielded no imaginary frequency, confirming that both structures correspond to equilibrium geometries. Molecular electrostatic potential map (MESP) and NPA charge analysis showed that A is zwitterion (TBD-CO_2 adducts) and B is TBD-CO_2 complex.

Furthermore, the transition state optimization, and reaction path following for TBD-CO_2 complex to zwitterion TBD-CO_2 adduct conversion was carried out at the same level to determine the reaction barrier and other parameters.

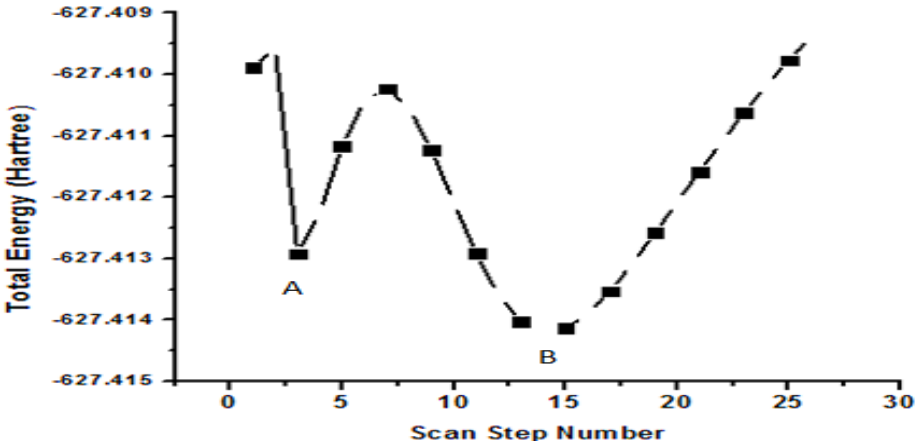

Figure 4 PES scan for TBD-CO_2 system at B3LYP/6-31G (d) level in gas phase (by varying internuclear distance between C1 of CO_2 and N14 of TBD) (A = TBD-CO_2 adduct and B = TBD-CO_2 complex).

The optimized structures for TBD-CO_2 complex, TS and TBD-CO_2 adduct are presented **Figure 2**. The theoretical calculations at B3LYP/6-31G (d) in gas phase predicted that TBD-CO_2 complex to TBD-CO_2 conversion reaction is endothermic. It was also reported that this adduct formation can be used as a post-combustion CO_2 capture-release system. Recently, an investigated the reaction of TBD with CO_2 to form the zwitterionic adduct by X-ray diffraction analysis and computational methods (DFT). According to this group report, CO_2 and tolylisothiocyanate undergo addition to TBD to form a formal zwitterion adduct [26, 27]. Our DFT results also support the formation the zwitterion. Therefore, one can easily conclude that along the reaction pathway of CO_2 with TBD, zwitterionic TBD-CO_2 adduct is one of the possible intermediate. In mechanism 1, we have investigated that this adduct is responsible for ring opening of aziridine in this mechanism for the formation of intermediate (IM).

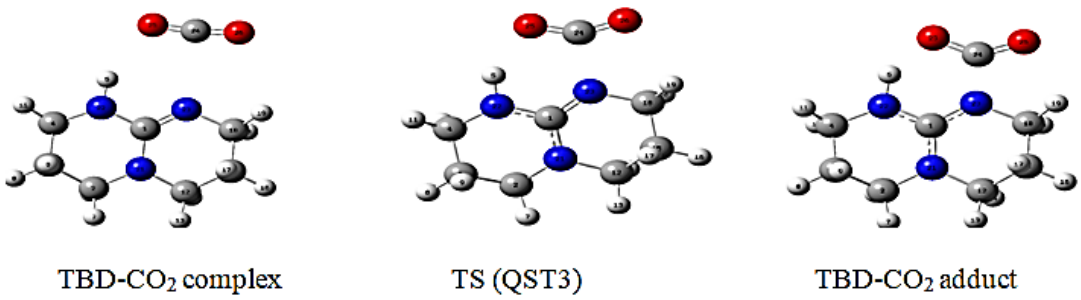

Figure 5 The optimized structure for TBD-CO_2 complex, TS and TBD-CO_2 adduct at B3LYP/6-31G (d) level.

LUMO of CO_2 is mostly centered on the carbon atom as depicted in **Figure 3**. Accordingly, CO_2 is typically electrophilic reagent; its interaction with nucleophile/ an electron-rich species is an efficient way for capture, activation and further transformation. The bond angle of CO_2 is 180° in Free State and its value in the TBD-CO_2 complex is determined to be 173.204° at B3LYP/6-31G (d). In the case of zwitterion, the bond angle of CO_2 is reduced to 134.773° upon interaction with TBD. The molecular electrostatic potential (MESP) yields information on the molecular regions that are preferred or avoided by an electrophile or nucleophile [71, 73]. The molecular electrostatic potential (MESP) for TBD-CO_2 complex, TS and TBD adduct at B3LYP/6-31G (d) level (Iso value = 0.004) are shown in **Figure 5**. The molecular electrostatic potential (MESP) of TBD-CO_2 complex show that region of N14 of TBD is red whereas C1 of CO_2 is blue. The red and blue regions in the MESP map of TBD-CO_2 complex refer to the negative and positive potential and correspond to electron rich and electron-deficient regions, respectively. As a result, N14 of TBD is susceptible for electrophilic attack and C1 of CO_2 is susceptible for a nucleophilic attack. From **Table 2**, the electronic chemical potential of TBD, $\mu = -1.91$ eV, is higher

than that of CO_2, $\mu = -4.627$ eV; suggesting that along TBD-CO_2 adduct formation reaction, the global electron density transfer (GEDT) [83] would be take place from TBD to CO_2. The GEDT concept comes from the observation that the electron density transfer from a nucleophile to an electrophile along a polar reaction is a global process, depending on the electrophilic/ nucleophilic interactions taking place between them. The global electron density transfer from the TBD (nucleophile) to the CO_2 (electrophile) is determined by the GEDT value at the TS of the reaction. The predicted global electron density transfer is found to be 0.228 electrons; the larger GEDT at the TS is the more polar the reaction is. Inspections of NPA charges on TBD-CO_2 adduct (supplementary information table S3) also show that upon interaction of CO_2 with TBD, the electron density on O25 of CO_2 found to be enhanced. Analysis of MEP as presented in **Figure 5** clearly support this again and show that CO_2 moiety of TBD-CO_2 adduct is nucleophilic center.

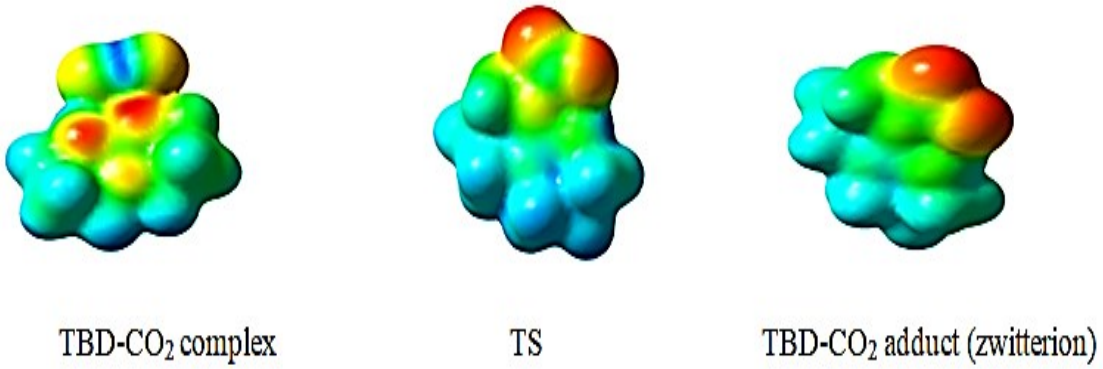

Figure 6 The molecular electrostatic potential (MESP) mapped on top of van der Waals surface for TBD-CO_2 complex, TS and TBD adduct at B3LYP/6-31G(d) level (Isovalue = 0.004).

Step II: The ring opening of aziridine with CO_2 moiety of TBD-CO_2 adduct

As revealed by NPA and MEP, the structure of adduct is quite differ from that of TBD-CO_2 complex arising from optimization of TBD and CO_2 together when the 2 species are 4 Å apart. We decided to extend the reactivity of the electron rich species, the TBD-CO_2 adduct, for the aziridine ring opening, using this adduct as a Lewis base. We demonstrated here that this adduct is efficient catalyst system in facilitating the ring opening of aziridine to give intermediate.

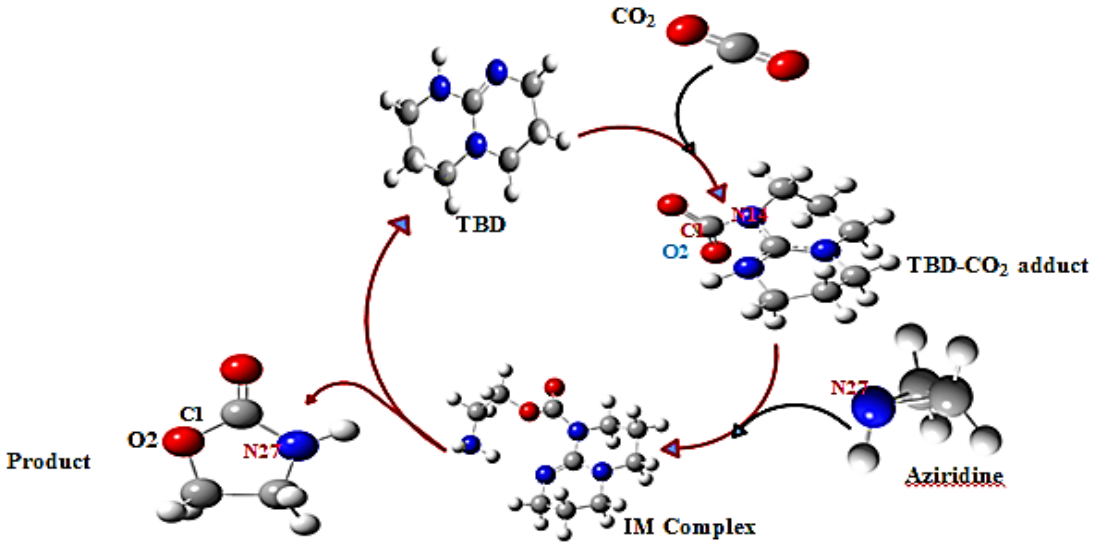

Figure 7 Proposed pathway (mechanism 1) for TBD-catalyzed cycloaddition reaction of CO_2 with aziridine.

Step III: Ring closure

The ring closure steps were formed in intermediate molecule of TBD- aziridine-CO_2 complex. The aziridine-CO_2 complex and TBD were also optimized together and we denote the optimized structure as Intermediate complex (IM). Then bond formed between N27 of aziridine and C1 of Carbon dioxide molecule to form final products. The thermodynamic and kinetic data for the ring opening step of mechanism 1 is presented in below **Table 4**.

Table 4 Kinetic and thermodynamic data for TBD catalyzed reaction in both gas phase and water (SMD) at 298.15 K and 1 atm.

Kinetic						
		$\Delta E^{\neq}$	$\Delta H^{\neq}$	$\Delta G^{\neq}$	$\Delta S^{\neq}$	k(T)
Gas phase	RC→IM(TS1)	46.335	46.336	48.716	−7.987	1.20×10^{-23}
	IM→PC(TS2)	32.084	32.078	34.683	−8.719	2.33×10^{-13}
Water	RC→IM(TS1)	15.883	15.883	21.277	−18.092	1.57×10^{-3}
	IM→PC(TS2)	24.837	24.837	26.977	−7.176	1.04×10^{-7}
Thermodynamic						
		ΔH	**ΔG**	**ΔS**	**(Keq)**	
Gas phase	RC→IM	−11.111	−8.9997	−7.102	3.96×10^{6}	
	IM→PC	−15.862	−17.169	4.403	3.86×10^{12}	
water	RC→IM	−17.632	−11.468	−20.675	2.55×10^{8}	
	IM→PC	−14.002	−15.505	5.044	2.33×10^{11}	

The ring opening of aziridine by TBD-CO_2 adduct (formation of IM through transition state 1 (TS1) in gas phase has activation barrier of 46.34 kcal/mol and Gibbs free energy of activation is 48.716 kcal/mol. Whereas computed energy barrier for intramolecular ring closure cyclization reaction through TS2 is predicted to be 32.084 kcal/mol and Gibbs free energy of activation for this step is 34.683 kcal/mol computed at B3LYP level with 6-31G (d) basis set. DFT at B3LYP/6-31G(d) level predicted the first step as the rate determine step for this mechanism in gas phase. **Figure 8** shows the energy profile for TBD catalyzed reaction for mechanism 1 both in gas phase and aqueous medium together with the optimized structures of pre-reactant complex, intermediate, transition state and product complex (gas phases is solid line and aqueous phase in broken line).

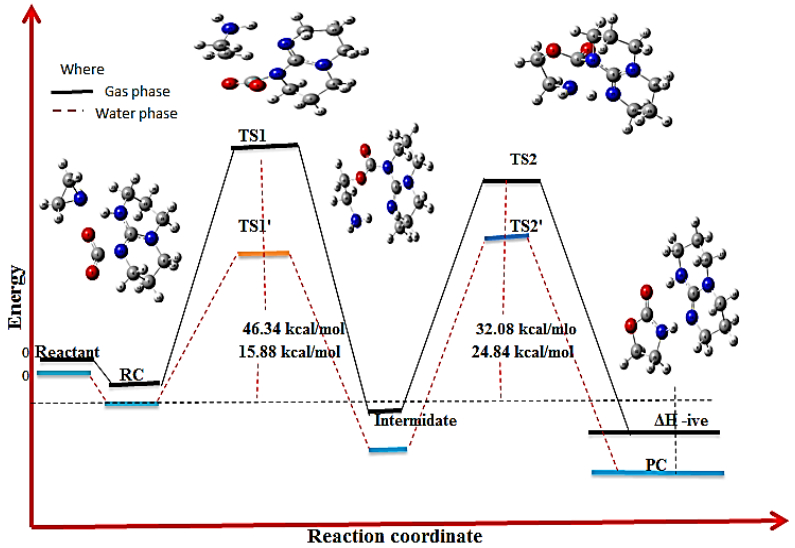

Figure 8 Energy profile for TBD catalyzed (mechanism 1) for the reaction of aziridine with CO_2 (Solid line = gas phase and broken line = aqueous phase) (RC = pre-reactant complex and PC = product complex). Energies are in kcal/mol.

The calculated Gibbs free energy changes for the ring opening step (RC→IM) and ring closure step (IM→PC), respectively are −8.99 and −17.167 kcal/mol in gas phase; indicating that the forward reaction is spontaneous and thermodynamically favored. The enthalpy change computed for RC→IM and ring IM→PC transformations are −11.11 and −15.86 kcal/mol, respectively. In this table, the activation barrier for the formation of IM from RC and formation of PC from IM, calculated in aqueous solution (using SMD solvent model) are 15.88 and 24.84 kcal/mol, respectively. Our calculations in aqueous solutions reveals that the rate determining step is now reversed; indicating the second step as the rate determining compared to gas phase. As indicated in the table, the activation barrier for forward reaction in water is largely reduced compared to gas phase. The activation barrier for forward reaction is large in gas phase and consequently their rate constant becomes very small. Therefore, these small rate constant values indicate that the forward reactions are kinetically slow in gas phase. But in water (SMD model), the formation of product is the rate determine step with activation energy of 24.84 kcal/mol. In conclusion, small value of activation energy and large value of equilibrium constant indicate that the forward reaction fast (kinetically favorable) in water.

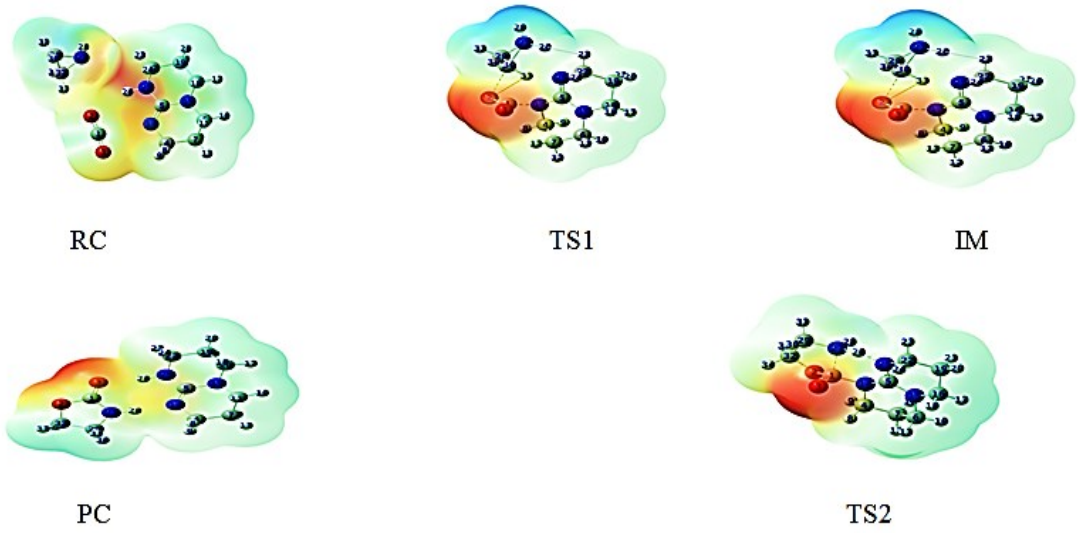

Figure 9 The molecular electrostatic potential (MESP) surface of RC, IM, PC, TS1 and TS2.

Selected transition state structure for mechanism 1: For the RC→IM transformation, only 1 large imaginary frequency (499.31 icm^{-1}) was found at the transition state (TS1) in gas phase. Similarly, for IM→PC process only 1 imaginary frequency was found (1205.36 icm^{-1}) at TS2 in gas phase. The presence of exactly one imaginary frequency confirms also that the structure is actually a transition state structure (**Figure 9**).

Table 5 Selected optimized parameters of TS1 for IM formation from RC and PC formation from IM through TS2 catalyzed by TBD in gas phase at 298.15 K temperature and 1 atm.

Bond length (Å)	RC→IM			IM→PC		
	RC	TS1	IM	IM	TS2	PC
C32-O2	3.1086	2.1811	1.4619	1.462	1.4233	1.4593
C32-C29	1.513	1.0797	1.1046	1.5356	1.5728	1.543
C29-N27	1.4961	1.4781	1.4825	1.4825	1.4709	1.4897
C1-O2	1.2323	1.2659	1.3738	1.3733	1.4648	1.4012
C1-N14	1.5701	1.542	1.4082	1.4081	1.5354	4.3173
N27-H26	2.8761	1.0227	1.0253	1.0253	1.2397	2.6614
N25-H26	1.0627	2.3005	2.4719	2.4722	1.3358	1.0282

As shown in **Table 5**, some selected transition state (TS) structure, for the 2 steps of mechanism 1 optimized at B3LYP/6-31G (d) level in gas phase. In the optimized geometry of the TS1, Ongoing from RC to IM, C32-O2 bond decrease from 3.1086 to 1.4619 Å. This indicates that N25-H26 bond being broken is elongated from 1.0627 to 2.4719 Å. In the product complex formation pathway through transition state (TS2), C1-N14 bond is stretched from 1.4081 to 4.3173 Å. But N25-H26 bond being formed is decreased from 2.4722 to 1.0282 Å.

Reaction mechanism 2

To begin this mechanism, the potential energy scan (PES) using redundant coordinate was carried out to explore the interaction between aziridine and CO_2 at B3LYP/6-31G(d) level in gas phase. Only 1 valley was observed as shown in **Figure 10**, confirming the existence of one equilibrium structure. The equilibrium structure obtained from PES was further investigated by optimizing at the same level and we obtained the interacting aziridine-CO_2 complex (Az-CO_2) as depicted in **Figure 11**. But we couldn't find the zwitterion structure for aziridine and CO_2 combination at this level.

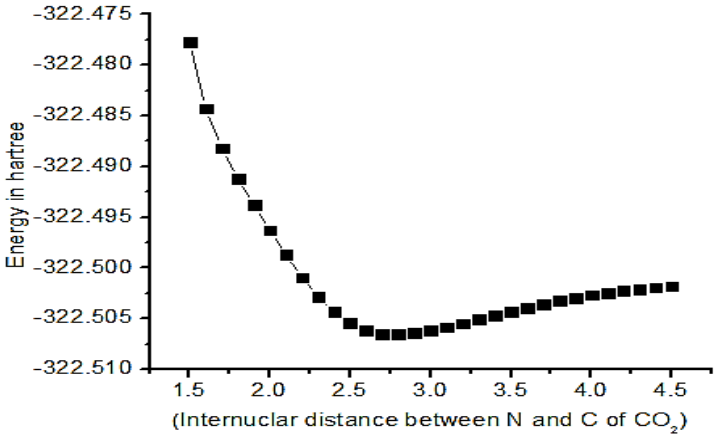

Figure 10 PES scan at the B3LYP/6-31G (d) level in gas phase (by varying internuclear distance between C of CO_2 and N of Az).

We started the investigation of mechanism 2 from aziridine-CO_2 complex (Az-CO_2). The aziridine-CO_2 complex and TBD were also optimized together and we denote the optimized structure as reactant complex (RC). This mechanism has 2 steps: First N22 of TBD attack aziridine-CO_2 complex at the C6 position, which leads to ring opening of the aziridine to form the intermediate IM (step 1); and subsequent intramolecular ring closure reaction to form 2-oxazolidinone by regenerating the TBD (step 2).The intermediate formed during ring opening is stabilized by removing H34 of TBD. In this case, an intermolecular hydrogen bond between the hydrogen atom bound to O10 and the nitrogen atom N33 is formed.

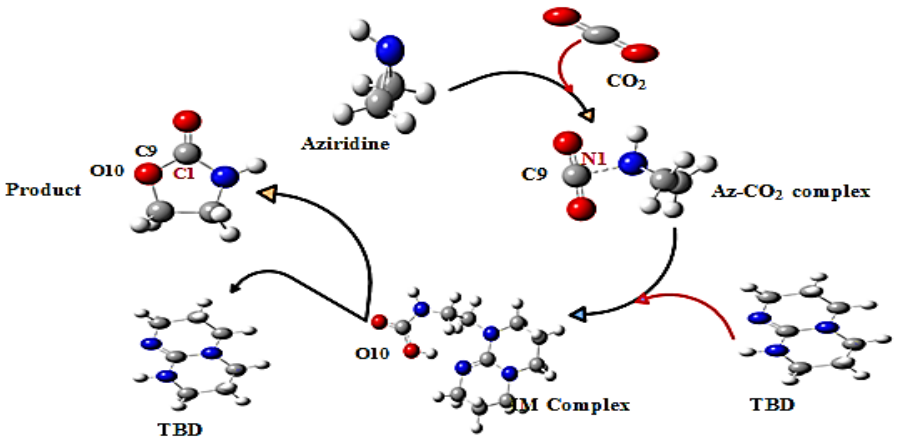

Figure 11 Proposed pathway (mechanism 2) of TBD-catalyzed cycloaddition reaction of aziridine with CO_2.

Kinetic and thermodynamic data for TBD catalyzed reaction of aziridine with CO_2 (mechanism 2)

Thermodynamic and kinetic parameters calculated at B3LYP/6-31G (d) level is given in **Table 6**. Energy profile for TBD catalyzed reaction (mechanism 2) of azaridine and CO_2 are presented in **Figure 10**. According to the data in **Table 6**, the activation energies for the formation of intermediate from reactant complex (RC) via TS1 and formation of product complex (PC) through TS2 are 24.81 and 45.285 kcal/mol, respectively in gas phase. Thus, the second step is rate determine step for this mechanism and demonstrated by the imaginary frequency of 504.43 icm^{-1} via TS2. The rate constant calculated for this step (step 2) is small, 3.93×10^{-21} s^{-1}.

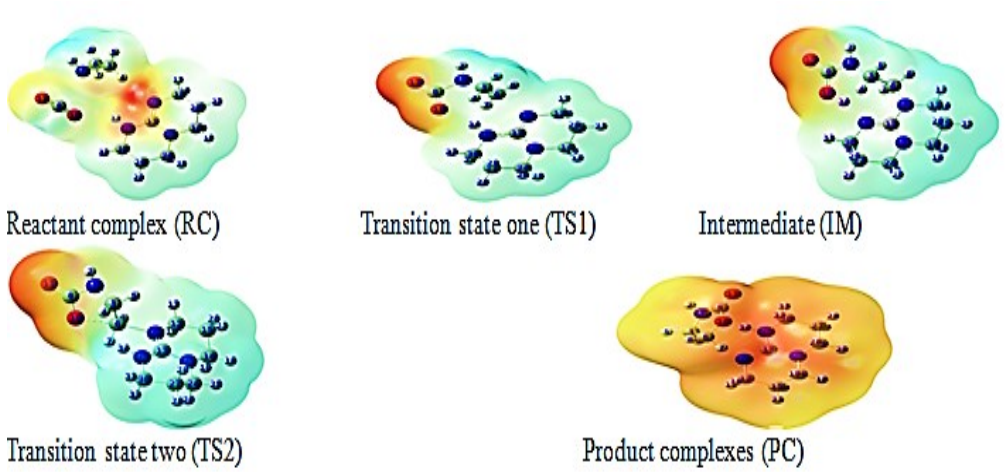

Figure 12 The molecular electrostatic potential (MESP) map for TBD catalyzed reaction of aziridine with CO_2 in gas phase at B3LYP/6-31G (d) level.

The ΔH value for intermediate formation is large negative (−23.303 kcal/mol in gas phase and −33.58 kcal/mol in water) and again the activation barrier for PC formation from intermediate step is higher (45.285 kcal/mol in gas phase and 33.045 kcal/mol in water) compared to the first step. The large negative ΔH value and high activation barrier for this step could be attributed to the existence of intramolecular hydrogen bonding in the intermediate.

Table 6 Kinetic and thermodynamic data for TBD catalyzed reaction (mechanism 2) of aziridine with CO_2 in both gas and water at 298.15 K temperature.

Kinetic data						
	Δ (change)	**$\Delta E^{\neq}$**	**$\Delta H^{\neq}$**	**$\Delta G^{\neq}$**	**$\Delta S^{\neq}$**	**k(T)**
Gas phase	RC→IM(TS1)	24.805	24.805	32.709	−26.512	6.54×10^{-12}
	IM→PC(TS2)	45.285	45.285	45.285	2.574	3.93×10^{-21}
Water	RC→IM(TS1)	8.6546	8.655	13.951	−17.764	3.68×10^{-2}
	IM→PC(TS2)	33.045	33.045	32.4002	2.161	1.10×10^{-11}
Thermodynamic						
			ΔH	**ΔG**	**ΔS**	**(Keq)**
Gas phase	RC→IM		−23.303	−14.663	−28.979	5.61×10^{10}
	IM→PC		3.310	0.699	8.757	3.25
Water	RC→IM		−33.58	−26.914	11.1587	5.37×10^{19}
	IM→PC		7.633	4.37876	10.913	6.15×10^{-4}

As easily seen from **Table 6**, intermediate formation reaction is spontaneous and thermodynamically favored reaction with Gibbs free energy change of −14.663 kcal/mol in gas phase and −26.914 kcal/mol in water. But for this mechanism, formation of product and regeneration of TBD from intermediate is non-spontaneous reaction. Thus, the first step is exothermic, releasing heat of −23.303 kcal/mol in gas phase and −33.58 kcal/mol in water while the second step is endothermic, requires heat of 3.31 kcal/mol in gas phase and 7.633 kcal/mol. Overall reaction is exothermic reaction and totally releases heat of −19.99 kcal/mol in gas and −25.947 kcal/mol in water.

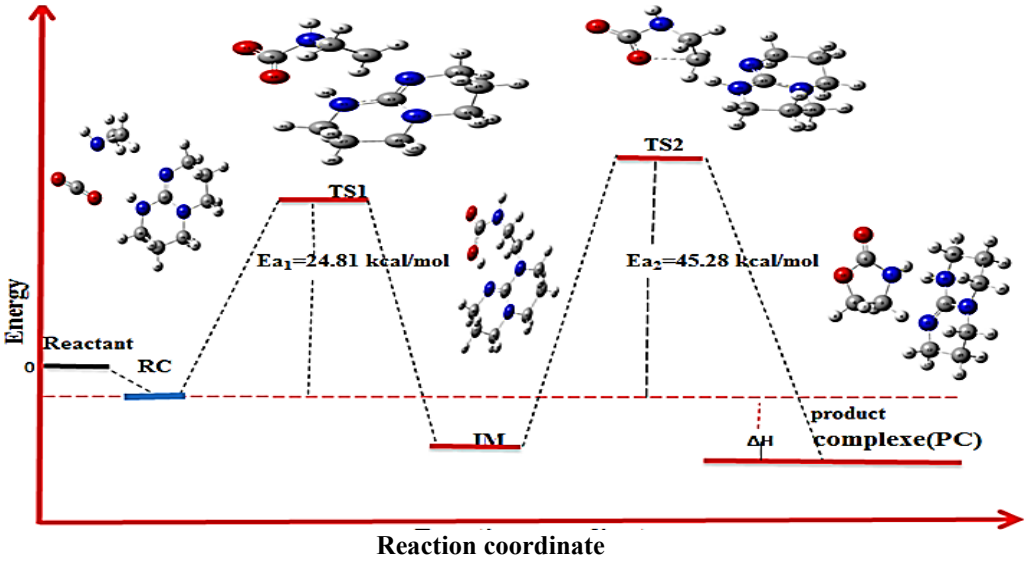

Figure 13 Energy profile for TBD catalyzed reaction (mechanism 2) of azaridine and CO_2 (energy in kcal/mol) selected geometric parameters for TS_1 and TS_2 of mechanism 2 in gas phase.

Table 7 Selected optimized parameters for IM formation from RC through TS1 and for PC formation from IM through TS2 catalyzed by TBD organocatalyst in gas phase at 298.15 K temperature.

	RC→IM				IM→PC		
Bond length (Å)	**RC**	**TS1**	**IM**		**IM**	**TS2**	**PC**
C6-N22	3.7331	2.2138	1.4877	C6-N22	1.4877	1.8804	3.0566
C3-C6	1.5077	1.4612	1.5489	C3-C6	1.5489	1.5242	1.5422
C9-O10	1.208	1.2499	1.3528	C6-O10	3.3406	2.0665	1.4689
C1-C9	1.6708	1.5374	1.4069	C9-O10	1.3528	1.2906	1.3936
O10-H3	1.9738	2.0726	1.0293	Bond Angle			
N33-H34	1.0401	1.0198	1.9038	C3-C6-N1	110.9033	107.812	102.9429

Ongoing from RC to IM, the C6-N22 bond length is reduced from 3.73 to 1.489 Å. This is confirmed by TS1, the unique imaginary frequency was 519.55 icm^{-1}, corresponded to the stretching vibration frequency of C6 relative to N22 and C6 relative to N1 of which indicate that opening of aziridine ring. Proton H34 moved from TBD molecule to the aziridine-CO_2 complex evolved in intermediate. During that the bond formed between O10-H34 and bond broken between N33-H34. The variation in bond angle depends on the electro negativity of the central atom, the presence of lone pair of electrons and the conjugation of the double bonds. Thus the bond angle in aziridine ring between atoms of C3-C6-N1 is 110.9° during intermediate formation, which decreased to 102.9° in the formation of product complex.

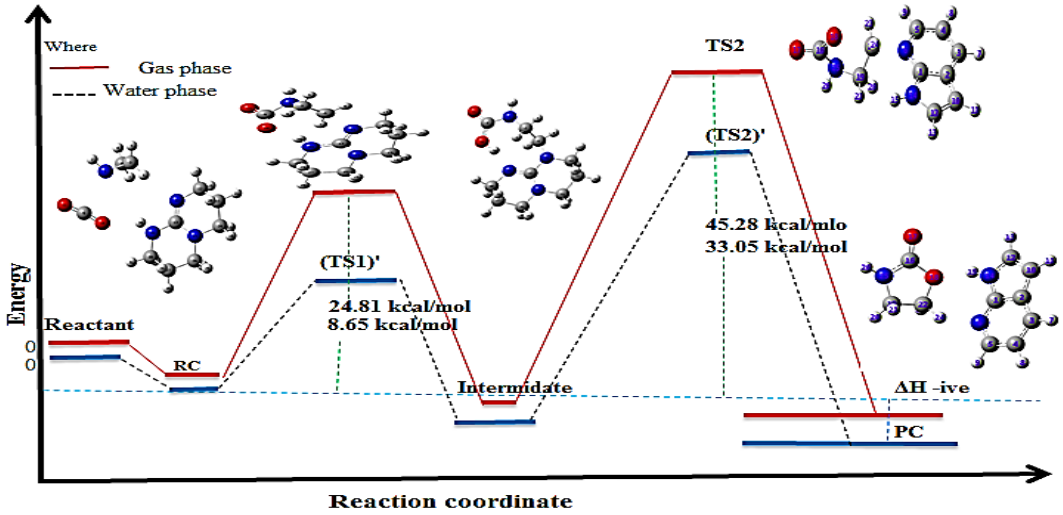

Figure 14 The calculated potential energy profile for mechanism 1 catalyzed by TBD reaction for aziridine with CO_2 in both gas and water.

Generally, from the above 2 TBD catalyzed reaction mechanism, the first reaction mechanism (TBD-CO_2 adduct) is most favored one in water (SMD model) with rate determine step activation energy of 24.84 kcal/mol in second step pathway. But in gas phase, the favored mechanism is the second one (Az-CO_2 complex mechanism) with rate determine step activation barrier of 45.28 kcal/mol in second step pathways.

Cycloaddition reaction of aziridine with CO_2 in the presence 7-azaindole (7-AZ) organocatalyst

Encouraged by the successful results of CO_2 fixation catalyzed by TBD, we next examined the cycloaddition reaction of CO_2 with aziridine using 7-aziandole as a catalyst. We also proposed 2 mechanisms for coupling reaction of aziridine with CO_2 assisted by 7-azaindole as shown in **Figures 15** and **19**.

Reaction mechanism 1

This mechanism has 2-step pathways: The ring opening of aziridine and intramolecular cyclization of intermediate to generate the product and 7-AZ. Initially, PES was carried out by varying internuclear distance between N atom aziridine and C of CO_2.

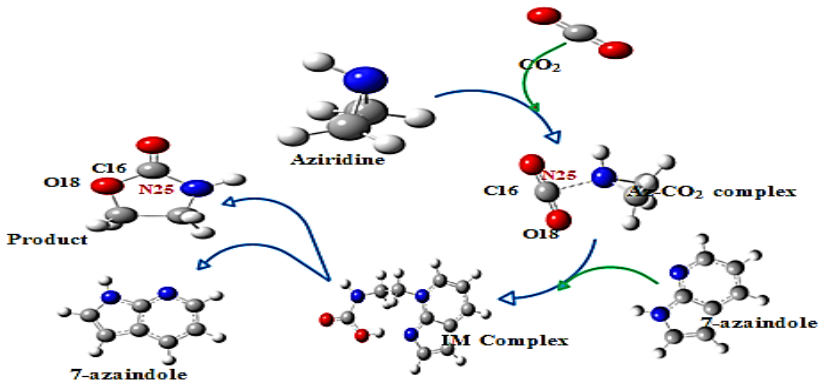

Figure 15 Possible pathways for 7-azaindole catalyzed cycloaddition reaction of aziridine with CO_2.

The structure from the minimum was taken and further optimized at the same level of theory. We obtained aziridine-CO_2 (Az-CO_2) complex as given in **Scheme 5** instead of aziridine-CO_2 adduct. **Table 8** presents kinetic and thermodynamic data for 7-azaindole catalyzed reaction of aziridine with CO_2 at

B3LYP/6-31G (d) level (mechanism 1) in gas phase and in water. Energy profile for 7-AZ catalyzed reaction for this mechanism can give in **Figure 13**. In the first step of this mechanism, free 7-azaindole plays a role as the catalyst precursor to promote the initial ring opening of activated aziridine from Az-CO_2 complex to form stable intermediate (IM). In this step, the ring opening of activated aziridine by 7-azaindole is accompanied by proton transfer from N-H of 7-AZ to O of CO_2; here 7-AZ is acting as proton donor. Thus, the presence of N-H group on 7-azaindole played a crucial role. This IM is more stable than the reactant complex (RC) and the formation of this intermediate is exothermic with enthalpy value of −11.5474 kcal/mol. The higher stability of this intermediate could be due to the presence of intramolecular hydrogen bonding (O-H…N).

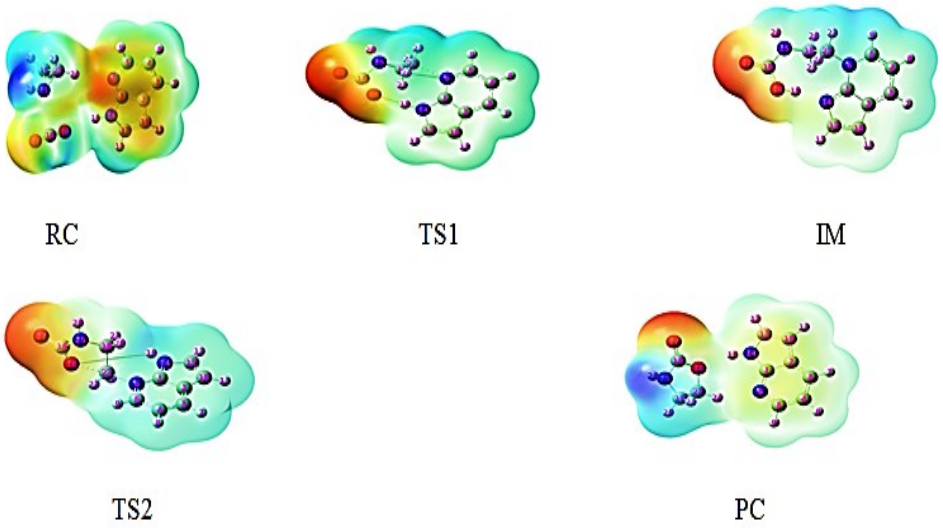

Figure 16 The molecular electrostatic potential (MESP) map for the 7-azaindole catalyzed reaction of aziridine with CO_2 in gas at B3LYP/6-31G (d) level (mechanism 1).

Table 8 Kinetic and thermodynamic data for 7-azaindole catalyzed reaction of aziridine with CO_2 at B3LYP/6-31G (d) level of theory in gas at 298.15 K temperature (mechanism 1).

Kinetic data						
	Δ(change)	**$\Delta E^{\neq}$**	**$\Delta H^{\neq}$**	**$\Delta G^{\neq}$**	**$\Delta S^{\neq}$**	**k(T)**
Gas phase	RC→IM (TS1)	26.7144	26.7144	35.6557	−29.989	4.52×10^{-14}
	IM→PC (TS2)	42.6343	42.6343	42.377	0.863	5.34×10^{-19}
Water	RC→IM (TS1)	10.7091	10.7091	15.9494	−17.579	1.26×10^{1}
	IM→PC (TS2)	28.9282	28.9288	27.4103	5.091	5.01×10^{-8}
Thermodynamic						
			ΔH	**ΔG**	**ΔS**	**(Keq)**
Gas phase	RC→IM		−11.547	−2.8012	−29.334	1.13×10^{2}
	IM→PC		−9.3223	−5.8498	9.178	1.94×10^{4}
Aqueous phase	RC→IM		−25.387	−18.089	−24.478	1.82×10^{13}
	IM→PC		−2.7686	−6.2193	11.574	3.62×10^{4}

Note: All energy values in kcal/mol, ΔS in cal/mol·K and rate constants in $s^{-1.}$

The gas phase calculated activation energies for IM formation and intramolecular cyclization reactions are 26.71 and 42.63 kcal/mol, respectively, indicating the cyclization as the rate determining step. The activation energy calculated for IM formation process was found to be less than that of the second step. The higher activation barrier for the second step could be also explained due to stability of IM, this is due to the existence of hydrogen bonding.

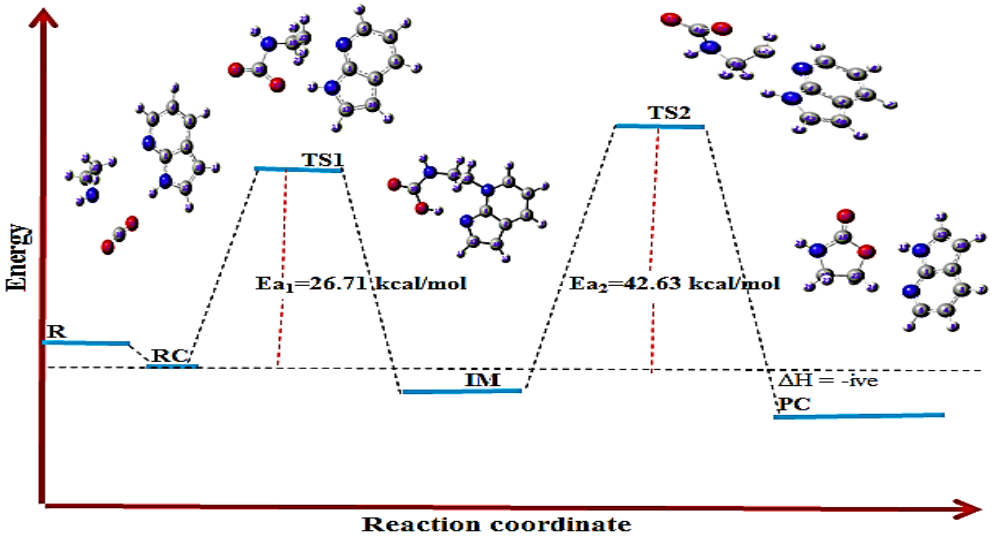

Figure 17 The energy profile for 7-AZ catalyzed reaction of aziridine with CO_2 along reaction coordinates in gas phase.

As can be seen from the table, the forward reaction is exothermic with the calculated values of ΔH for IM and PC formations are −11.547 and −9.3223 kcal/mol, respectively. Similarly, the corresponding enthalpy changes RC→IM and IM→PC for transformations, respectively are −25.387 and −2.7686 kcal/mol in water. The computed values of ΔH, ΔG and equilibrium constant (Keq) indicate that the reaction is exothermic, spontaneous and thermodynamically favored.

Table 9 Some selected geometry bond length for formation IM through TS1 and formation of product through TS2 in gas phase at 298.15 K temperature.

RC→IM				IM→PC			
Bond length (Å)	**RC**	**TS1**	**IM**	**Bond length (Å)**	**IM**	**TS2**	**PC**
C22-N6	3.3431	2.12	1.487	C22-N6	1.487	1.799	3.2821
C22-N25	1.5043	1.886	2.4728	C22-C19	1.5524	1.5281	1.543
C16-N25	1.6712	1.53	1.4147	C16-N25	1.4147	1.4468	1.408
O18-H15	1.9388	1.781	1.0405	O18-H15	1.0405	4.1466	2.0345
N14-H15	1.0186	1.038	1.8112	N14-H15	1.8112	1.011	1.0158

The result shown in **Table 9** indicate that, the bond lengths between C22-N25 and N14-H15 are broken and elongated from 1.5043 and 1.0186 Å in reactant complex to 2.4728 and 1.8112 Å in formation of intermediate respectively. But this bond distance can decrease during formation product complex though TS2. Similarly, in the PC formation pathways from IM through transition state (TS2), the bond lengths can be shorter that is from C22-N6 was 3.3431 to 1.487 Å, C16-N25 is 1.6712 to 1.4147 Å and O18-H15 is 1.9388 to 1.0405 Å.

Solvent effects on 7-azaindole catalyzed reaction of aziridine with CO_2

All structures of transition states and stationary state have re-optimized in water (SMD model). Our ΔH calculation showed that the stability gained for formation of intermediate and product formation in water as a polar solvent (ε = 78.39) were −25.387 and −2.77 kcal/mol, respectively. The optimized geometries of the transition state structures in solvent show that activation energies value of 10.7091 and 28.93 kcal/mol, respectively. This result in water being a polar protic solvent stabilizes the polar transition state more than the gas phase transition state. The overall reaction is found to be exothermic

with −20.87 kcal/mol gas phase. Due to the solvation of polar product of water reaction is highly exothermic with −28.16 kcal/mol.

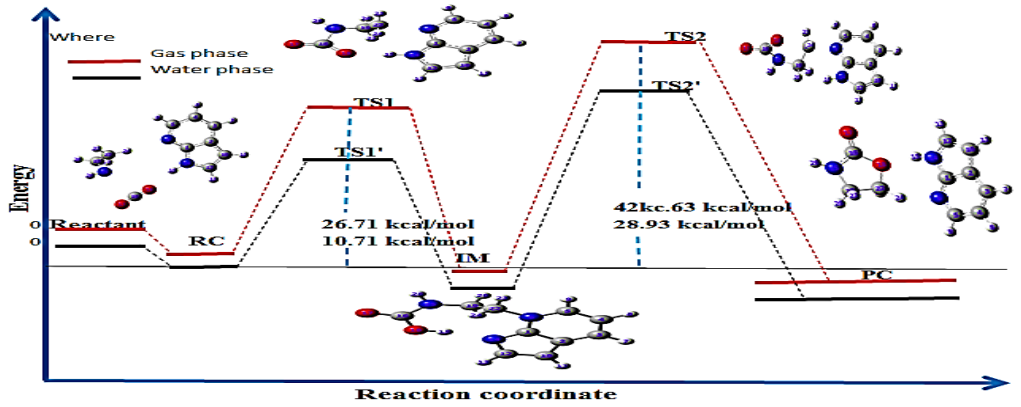

Figure 18 potential energy profiles for 7-azaindole catalyzed reaction of aziridine with CO_2 along reaction coordinates in both gas and water phase.

Reaction mechanism 2

This mechanism has also 2-steps: The ring opening of aziridine by 7-AZ…CO_2 complex and intramolecular cyclization of intermediate to generate the product and 7-AZ. Initially, PES was carried out by varying internuclear distance between N atom of 7-Az and C of CO_2. Only one minimum was obtained as shown in supplementary information **Figure 1**. The structure from the minimum was taken and further optimized at the same level of theory. We obtained 7-AZ-CO_2 complex as given in **Figure 19** instead of zwitterionic 7-AZ-CO_2 adduct. **Table 11** presents kinetic and thermodynamic data for 7-azaindole catalyzed reaction of aziridine with CO_2 at B3LYP/6-31G (d) level (mechanism 2) in gas phase and in water. Energy profile for 7-AZ catalyzed reaction for this mechanism is given in **Figure 15**. In the first step of this mechanism, O of CO_2 moiety from 7-AZ…CO_2 complex assisted the ring opening of aziridine to form stable intermediate (IM). In this step, the ring opening of aziridine is accompanied by proton transfer from N-H of 7-AZ to N of aziridine; here 7-AZ is acting as proton donor. Thus, the presence of N-H group on 7-azaindole played a role to open the aziridine ring. In the second step (ring closure step), proton from nitrogen atom of aziridine to nitrogen atom of 7-azaindole has occurred. During this reaction 7-azaindole can act as proton accepter.

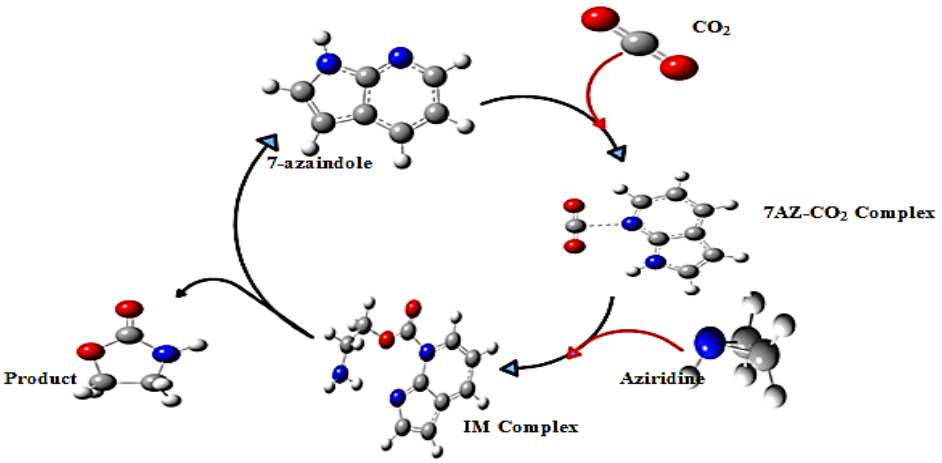

Figure 19 Proposed pathway (mechanism 2) for cycloaddition reaction of aziridine with CO_2 catalyzed by 7-azaindole.

The intermediate complex was formed by a proton transfer reaction from 7-azaindole to nitrogen atom of aziridine. During this reaction, 7-azaindole reaction can act as proton donor compound. The second transition state can be formed by back donation of proton from nitrogen atom of aziridine to nitrogen atom of 7-azaindole. During the reaction 7-azaindole can act as proton accepter compound.

Table 11 Kinetic and thermodynamic data for 7-azaindole catalyzed reaction of aziridine with CO_2 in both gas and water phase at 298.15 K temperature (mechanism 2).

Kinetic data						
		$\Delta E^{\neq}$	**$\Delta H^{\neq}$**	**$\Delta G^{\neq}$**	**$\Delta S^{\neq}$**	**k(T)**
Gas phase	RC→IM (TS1)	58.133	58.134	64.463	−21.23	3.44×10^{-35}
	IM→PC (TS2)	11.8091	11.809	13.8811	−6.949	4.14×10^{2}
Water	RC→IM (TS1)	46.9208	46.921	52.8966	−8.33	1.04×10^{-26}
	IM→PC (TS2)	6.99234	6.9923	8.61885	−5.455	2.99×10^{6}
Thermodynamic data						
			ΔH	**ΔG**	**ΔS**	**(Keq)**
Gas phase	RC→IM		9.036	15.446	−21.499	4.75×10^{-12}
	IM→PC		−24.75	−27.165	8.075	8.21×10^{8}
Water	RC→IM		4.489	10.987	−21.795	8.82×10^{-9}
	IM→PC		−27.41	−29.075	5.589	2.06×10^{21}

Note: All energy in kcal/mol, ΔS in cal/mol·K and rate constants in s^{-1} in both gas phase and water (SMD model), the rate determine step is first step 1 (TS1) with the activation energies for RC→IM and IM→PC of 58.13 and 46.92 kcal/mol, respectively. These values are shown in **Figure 15**.

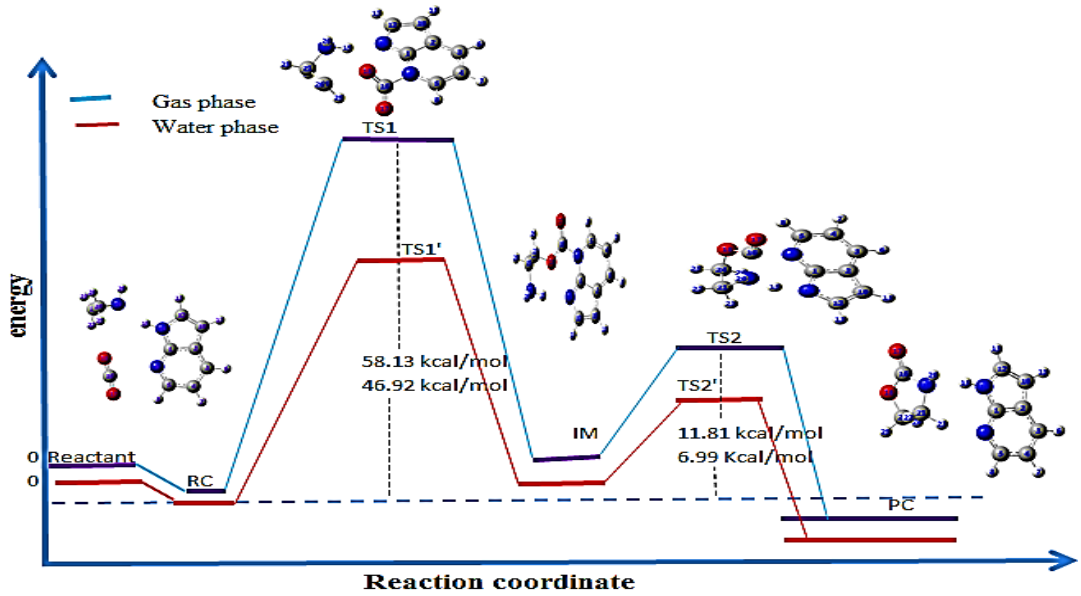

Figure 20 Energy diagram for 7-azaindole catalyzed reaction aziridine with CO_2.

As compare to reaction in gas phase, water reaction has minimum activation energy barrier by stabilize the chemical reaction. These decreases in activation energy indicate that rate of reaction become increase. The overall Gibbs free energy in gas phase and water were −11.71 and −18.09 kcal/mol, respectively. These negative values indicate that the given chemical reaction spontaneous and exothermic.

Conclusions

In the work of theoretically study on TBD and 7-azaindole catalyzed fixation of CO_2 with Aziridin to produce 2-oxazolidinone, DFT calculations reveal that mechanism 1 is the preferred reaction pathway for the TBD catalyzed coupling reaction of CO_2 with Aziridine in water using SMD solvent model. However, in the gas phase, the calculated kinetic data indicated that mechanism 2 is the favored pathway. The catalytic cycle of mechanism 1 is composed of the 3 major steps; these are Zwitterionic TBD-CO_2 adduct formation, Ring opening of aziridine facilitated by TBD-CO_2 adduct and intramolecular cyclization reaction to form the product and regenerate the TBD. In the favored mechanism catalyzed by TBD in water, TBD first interact with CO_2 to form TBD-CO_2 adduct (zwitterion) and then the zwitterion formed facilitated the ring opening of aziridine to form intermediate. In the case of 7-azaindole catalyzed reaction, mechanism 1 is the most favorable pathway in both gas phase and water. The effects of temperature on the thermodynamic and kinetic properties for 7-AZ catalyzed reaction were also investigated at 298.15, 400, 600, 800 and 1,000 K. It was found that the effect of temperature for the studied reactions didn't significantly change the thermodynamics and kinetic parameters. However, these parameters were significantly affected in the presence of water using SMD solvent model. In favored mechanism catalyzed by TBD, the first step is rate determine step with activation energy of 46.35 kcal/mol in gas phase but in water the second step is rate determine step with energy barrier of 24.83 kcal/mol. In the case of 7-azaindole catalyzed reaction, activation energy is small compared with TBD catalyzed mechanism and the calculated activation energies are 26.71 and 42.63 kcal/mol for step 1 (TS1) and step 2(TS2) in gas phase. The presence of N-H group in the fused-ring TBD and 7-azaindole assisted ring opening of aziridine to form stable intermediate and accelerate the chemical fixation of CO_2 with aziridine. Overall, the results from quantum calculations reveal that both TBD and 7-azaindole accelerated the coupling reaction of CO_2 with aziridine to produce 2-oxazolidinone compared to bare reaction.

Acknowledgements

Tesfaye Tadesse acknowledges Department of Chemistry, Hawassa University, Ethiopia for the grant support to successfully carry out of the project.

References

[1] N Ahmad and L Du. Effects of energy production and CO_2 emissions on economic growth in Iran: ARDL approach. *Energy* 2017; **123**, 521-37.
[2] S Sibilio, A Rosato, G Ciampi, M Scorpio and A Akisawa. Building-integrated trigeneration system: Energy, environmental and economic dynamic performance assessment for Italian residential applications. *Renew. Sustain. Energ. Rev. 2*017; **68**, 920-33.
[3] M Kahia, MSB Aïssa and C Lanouar. Renewable and non-renewable energy use-economic growth nexus: The case of MENA net oil importing countries. *Renew. Sustain. Energ. Rev.* 2017; **71**, 127-40.
[4] M Ahiduzzaman and AKMS Islam. Greenhouse gas emission and renewable energy sources for sustainable development in Bangladesh. *Renew. Sustain. Energ. Rev.* 2011; **15**, 4659-66.
[5] K Goto, K Yogo and T Higashii. A review of efficiency penalty in a coal-fired power plant with post-combustion CO_2 capture. *Appl. Energ.* 2013; **111**, 710-20.
[6] WH Chen, SM Chen and CI Hung. Carbon dioxide capture by single droplet using Selexol, Rectisol and water as absorbents: A theoretical approach. *Appl. Energ.* 2013; **111**, 731-41.
[7] K Sołtys-Brzostek, M Terlecki, K Sokołowsi and J Lewiński. Chemical fixation and conversion of CO_2 into cyclic and cage-type metal carbonates. *Coord. Chem. Rev.* 2017; **334**, 199-231.
[8] J Peng, Y Geng, HJ Yang, W He, Z Wei and J Yang. Efficient solvent-free fixation of CO_2 into cyclic carbonates catalyzed by Bi (III) porphyrin/TBAI at atmospheric pressure. *Mol. Catal.* 2017; **432**, 37-46.
[9] Y Zhang, Y Zhang, Y Ren and O Ramström. Synthesis of chiral oxazolidinone derivatives through lipase-catalyzed kinetic resolution. *J. Mol. Catal. B Enzym.* 2015; **122**, 29-34.
[10] ZZ Yang, LN He, J Gao, AH Liu and B Yu. Carbon dioxide utilization with C-N bond formation: Carbon dioxide capture and subsequent conversion. *Energ. Environ. Sci*. 2012; **5**, 6602-39.
[11] S Kim, H Shi and JY Lee. CO_2 absorption mechanism in amine solvents and enhancement of CO_2 capture capability in blended amine solvent. *Int. J. Greenhouse Gas Contr.* 2016; **45**, 181-8.
[12] MF Rojas, FL Bernard, A Aquino, J Borges, FD Vecchia and S Menezes. Poly(ionic liquid)s as

efficient catalyst in transformation of CO_2 to cyclic carbonate. *J. Mol. Catal. A Chem.* 2014; **392**, 83-8.

[13] M Azzi and S White. 20 - emissions from amine-based post-combustion CO_2 capture plants. *Woodhead Publish.* 2016; **2016**, 487-504.

[14] W Koch and MC Holthausen. *A chemist's guide to density functional theory.* 2nd ed. Wiely-VCH, Weinheim, Germany, 2000.

[15] BO Milhøj, ED Hedegard and SPA Sauer. On the use of locally dense basis sets in the calculation of EPR hyperfine couplings: A study on model systems for bio-inorganic Fe and Co complexes. *Curr. Inorg. Chem*. 2013; **3**, 270-83.

[16] A Łapczuk-Krygier, VY Korotaev, AY Barkov, VY Sosnovskikh, E Jasińska and R Jasiński. A DFT computational study on the molecular mechanism of the nitro group migration in the product derived from 3-nitro-2 (trifluoromethyl)-*2H*-chromene and 2-(1-phenylpropylidene)malononitrile. *J. Fluorine Chem.* 2014; **168**, 236-9.

[17] AV Marenich, CJ Cramer and DG Truhlar. Universal solvation model based on solute electron density and on a continuum model of the solvent defined by the bulk dielectric constant and atomic surface tensions. *J. Phys. Chem*. 2009; **113**, 6378-96.

[18] ELM Miguel, CIL Santos, CM Silva and JR Pliego. How accurate is the SMD model for predicting free energy barriers for nucleophilic substitution reactions in polar protic and dipolar aprotic solvents. *J. Braz. Chem. Soc.* 2016; **27**, 2055-61.

[19] LR Domingo, P Perez and JA Saez. Understanding the local reactivity in polar organic reactions through electrophilic and nucleophilic Parr functions. *RSC Adv.* 2013; **3**,1486-94.

[20] LR Domingo. A new C-C bond formation model based on the quantum chemical topology of electron density. *RSC Adv.* 2014; **4**, 32415-28.

[21] AE Reed, LA Curtiss and F Weinhold. Intermolecular interactions from a natural bond orbital, donor-acceptor viewpoint. *Chem. Rev.* 1988; **88**, 899-926.

[22] W Li, D Huang and Y Lv. Mechanism of N-heterocyclic carbene-catalyzed chemical fixation of CO_2 with aziridines: A theoretical study. *RSC Adv.* 2014; **4**, 17236-44.

[23] A Axelsson, A Antoine-Michard and H Sunden. Organocatalytic valorisation of glycerol via a dual NHC-catalysed telescoped reaction. *Green Chem*. 2017; **19**, 2477-81.

[24] C Sabot, KA Kumar, S Meunier and C Mioskowski. A convenient aminolysis of esters catalyzed by 1,5,7-triazabicyclo[4.4.0]dec-5-ene (TBD) under solvent-free conditions. *Tetrahedron Lett.* 2007; **48,** 3863-6.

[25] S Matsukawa, J Kimura and M Yoshioka. TBD or PS-TBD-catalyzed one-pot synthesis of cyanohydrin carbonates and cyanohydrin acetates from carbonyl compounds. *Molecule* 2016; **21**, 1030.

[26] JE Gómez and AW Kleij. Recent progress in stereoselective synthesis of cyclic organic carbonates and beyond. *Curr. Opin. Green Sustain.* 2017; **3**, 55-60.

[27] AA Chaugule, AH Tamboli and H Kim. Ionic liquid as a catalyst for utilization of carbon dioxide to production of linear and cyclic carbonate. *Fuel* 2017; **200**, 316-32.